YMTHE, Volume *28*

Supplemental Information

RBP EIF2S2 Promotes Tumorigenesis and Progression by Regulating MYC-Mediated Inhibition via FHIT-Related Enhancers

Jiwei Zhang, Shengli Li, Ling Zhang, Juan Xu, Mingxu Song, Tingting Shao, Zhaohui Huang, and Yongsheng Li

Supporting materials and methods

RNA pull-down assays and mass spectrometry analyses

LINC01600 or antisense-LINC01600 RNAs were transcribed and labelled by the Biotin RNA Labeling Mix (Roche, USA), treated with RNase-free DNase I (Takara, Japan) and purified with an RNeasy Mini Kit (QIAGEN, USA). Briefly, LINC01600 sequence was in vitro transcribed with biotin RNA-labeling mix and T7 RNA polymerase (Invitrogen) according to the manufacturer's instructions. The pre-treated biotinylated RNAs were incubated with 1mg protein extracts of HCT-116 cells at 4 °C for 1h, gently mixed with 40μl washed streptavidin beads (Invitrogen, USA) and incubated on a rotator overnight. The beads were washed briefly five times in 1× washing buffer (5mM Tris-HCl, 1M NaCl, 0.5mM EDTA, and 0.005% Tween 20). The proteins were precipitated and diluted in 60μl protein lysis buffer, separated by gel electrophoresis and visualized by silver staining. Specific bands were excised for proteomics screening by mass spectrometry analysis (Shanghai Applied Protein Technology, Shanghai, China).

RNA Immunoprecipitation assay

RNA Immunoprecipitation (RIP) assays were performed using the Magna RIP RNA-Binding Protein Immunoprecipitation Kit (Millipore). Briefly, cells growing in 15cm-dishes were lysed in 1.2ml of lysis buffer containing protease inhibitors and RNase Inhibitor (Thermo Fisher Scientific Inc., Rockford, IL, USA) and centrifuged at 12,000 r.p.m. for 30min. The supernatants were incubated with Protein G Dynabeads (Thermo Fisher Scientific, Carlsbad, California, USA), which were incubated with the indicated antibodies for 12h at 4°C with gentle rotation. The beads were washed thrice with wash buffer containing RNase inhibitor and then twice with PBS containing RNase inhibitor. The RNA was extracted using the Total RNA isolation kit (Thermo Fisher Scientific Inc), and qRT-PCR was performed as described in Supplemental Materials. For the RIP assays of deletion mutants, 5p mol plasmids with FLAG- or HA-tagged full-length and truncated EIF2S2, MYC were transiently transfected into HCT-116 cells, and the cell lysates were immunoprecipitated with indicated antibodies.

DNA and RNA isolation

Genomic DNA was isolated using the General AllgGen Kit (Cwbio, China) according to the manufacturer’s protocol. Total RNA was extracted using RNAiso reagent (Takara, Japan). The concentrations of DNA and RNA were determined using NanoDrop 2000 (Thermo, USA). Complementary DNA (cDNA) was synthesized using the PrimeScript RT reagent kit (TaKaRa,

Japan). qRT-PCR analyses were conducted to quantitate the relative mRNA expression using SYBR Premix Ex Taq (TaKaRa), with β-actin as an internal control. qRT-PCR assays were carried out using TaqMan probes (Applied Biosystems, USA). The reactions were incubated in 96- or 384-well optical plates at 95°C for 10 min, followed by 40 cycles of 95°C for 15 s and 60°C for 1 min. After the reactions, the cycle threshold (Ct) data were determined using default threshold settings, and the mean Ct was determined from the duplicate PCRs. A comparative ΔCt method was used to compare each condition with controls, and the values are expressed as $2-\triangle Ct$. The relative levels of mRNAs were normalized to U6, a ubiquitously expressed small nuclear RNA. All the primers were listed in Table S2.

Western blotting

Total protein was separated by 8% (or 10%) sodium dodecyl sulfate polyacrylamide gel electrophoresis and transferred to a PVDF membrane. After blocking with non-fat milk, the polyvinylidene difluoride membrane was incubated with a rabbit anti-human NOTCH1 antibody (1:1000, 20687-1-AP, Proteintech, USA) or a mouse anti-β-actin antibody (1:1000, AA128, Beyotime, China).

Northern blot

We used a NorthernMax Kit from Ambion (Thermo Fisher Scientific,Carlsbad, California, USA) and DIG Northern starter Kit (Roche, Indianapolis,Indiana, USA) with Digoxin-labelled RNA probes to detect LINC01600 in the HCT-116 and LoVo cells. Approximately 10μg of enriched polyA + RNA was loaded per lane for northern blot analysis, according to the manufacturer's instructions.

5′ and 3′ RACE assay

We used 5′ and 3′ RACE to determine the transcriptional initiation and termination sites of LINC01600 with a SMARTer RACE cDNA Amplification kit (Clontech, California, USA), according to manufacturer's instructions. The sequences for the gene-specific PCR primers used for 5′ and 3′RACE analysis are given in Table S2.

Subcellular fractionation

Cytoplasmic and nuclear fractions of HCT-116 cells were prepared and collected according to the instructions of the Nuclear/Cytoplasmic Isolation kit (Thermo Fisher Scientific, Carlsbad, California, USA). β-actin was used as the cytoplasmic endogenous control. U2 small nuclear RNA was used as the nuclear endogenous control.

Cell proliferation and colony formation assays

The cells were seeded in 96-well flat-bottomed plates, with each well containing 1500 cells in 100μl of cell suspension. After a certain time in culture, cell proliferation was quantified using the Cell Counting Kit-8 (CCK8; Dojindo Laboratories, Japan) according to the manufacturer's instructions. For the colony formation assays, 1000 cells of HCT-116, SNU-449, MGC-803 and 1500 cells of SGC-7901 and Huh-7 cells were plated into each well of 6-well plates and incubated in medium containing 10% FBS for 15 days. The colonies were fixed with methanol and stained with 0.1% crystal violet in 20% methanol for 20 min. The number of colonies containing more than about 30 cells was counted using an inverted microscope.

Invasion and migration assays

Invasion assays were performed in Millicell chambers in triplicate. The 8-μm pore inserts were coated with 30μg of Matrigel (BD Biosciences, Franklin Lakes, New Jersey, USA). The migration assay was conducted similarly, without coating filters with Matrigel. The cells (3×10^4) were added to the coated filters in serum-free medium. We added medium containing 10% FBS to the lower chambers as a chemoattractant. After 24 h at 37 °C in an incubator at 5% CO2, cells that migrated through the filters were fixed with methanol and stained with crystal violet. Cell numbers were counted in five random fields.

Luciferase assay

Approximately 5,000 HEK-293T cells or 10,000 CRC (HCT-116, LoVo) cells per well were plated into 96-well plates and were co-transfected with 50 nmol/L of siRNA (or NC), 50 ng of the luciferase reporter, and 10 ng of the pRL-CMV Renilla luciferase reporter using 0.5 μL Lipofectamine 2000 (Invitrogen, USA) per well. After 48-h of transfection, the luciferase activities were quantified using a dual-luciferase reporter assay (Promega, USA).

***In vivo* assays**

Female athymic BALB/c nude mice, aged 4–5 weeks old, purchased from the Experimental Animal Center of Shanghai Cancer Institute (Shanghai, China). Mice (10 in each group) were injected subcutaneously with 0.2 ml of cell suspension containing 5×10^5 cells (pWPXL-VECTOR and pWPXL-EIF2S2 stable LoVo cell line) in the right axilla. Tumor growth rates were monitored. When a tumor was palpable, it was measured every other day, and its volume was calculated according to the formula volume = length × width^{2}x0.5. Sample size was not predetermined for these experiments. In addition, an orthotopic mouse model was used to

evaluate the effect of EIF2S2 on hepatic metastasis. Briefly, 2×10^6 LoVo cells stably expressing EIF2S2 were injected into the submucosal tissue of cecum of an athymic male BALB/c nude mouse at 4-5 weeks of age (n=10 for each group). The number of metastatic foci in the liver, lung and intestine were determined using the hematoxylin eosin (H&E) (Beyotime Biotechnology) staining in tissue sections under a binocular microscope (Leica, Wetzlar Lottehaus, Germany). All experiments were performed in accordance with relevant institutional and national guidelines and regulations of Shanghai Medical Experimental Animal Care Commission.

RNA interference and generation of lentivirus particles

The sequences of small interfering RNA (siRNA) oligonucleotides targeting EIF2S2, LINC01600, MYC,FHIT and the negative control siRNA were purchased from RiboBio (RiboBio Biotechnology, Guangzhou, China). Transfections with siRNA (50 nM) were performed with Lipofectamine 2000. The human EIF2S2 sequence was cloned from HCT-116 cell cDNA and cloned into lentivirus expression vector pWPXL to generate pWPXL-EIF2S2 cells. The LINC01600 and FHIT expression vectors were constructed by inserting the respective sequences into pWPXL vector to generate pWPXL-LINC01600 and pWPXL-FHIT, respectively. The HEK293T cells were transfected with pWPXLEIF2S2, pWPXL-MYC, pWPXL-LINC01600 or pWPXL-FHIT, with the packaging and envelope plasmids psPAX2 and pMD2.G, respectively (gifts from Dr. Didier), using Lipofectamine 2000 (Invitrogen) according to the manufacturer's instructions.

Immunoblotting analysis

CRC Cells (5×10^6) were lysed for 30 min with lysis buffer (Beyotime Biotechnology) containing protease inhibitors (Roche, Indianapolis, IN, USA). The protein concentrations were determined by the BCA method (Pierce, Thermo Fisher Scientific Inc., Rockford, IL, USA). After centrifugation at 16,400×g for 15 min at 4 °C, the samples were resolved by SDS/PAGE, transferred to PVDF membranes (Immobilon-P membrane, Millipore, Massachusetts, USA), and analyzed by immune blotting using HRP-conjugated secondary antibodies. The membranes were blocked with 5% (wt/vol) skimmed milk in TBS plus Tween 20 at 4 °C overnight before probing with antibodies. Information on the antibodies are provided Supplementary Table 2. An enhanced chemiluminescent (ECL) chromogenic substrate was used to visualize the bands (Pierce). Visualization was performed using the Enhanced Chemiluminescence Plus Western Blotting Detection System (GE Healthcare, Connecticut, USA) and LAS-4000EPUV mini Luminescent Image Analyzer (GE Healthcare).

Immunohistochemistry

The expression levels of EIF2S2 and MYC protein were determined by immunohistochemistry (IHC) analysis using colorectal cancer tissue arrays constructed previously. IHC staining was performed on 4-mm sections of paraffin-embedded tissue samples. Briefly, the slides were incubated with an anti-EIF2S2 and anti-MYC antibody (CST, 1:200) at 4°C overnight. The subsequent steps were performed using the GTVision III Detection System/Mo&Rb (GeneTech, China).

***In vitro* cellular IC50 assays**

Vector and pWPXL-EIF2S2 LoVo cells and siNC, siEIF2S2 HCT-116 were seeded in 96-well flat-bottomed plates, with each well containing 5000 cells in 100 μl of cell suspension to determine the concentration that causes 50% inhibition of cell viability. According to the recommended concentrations of Oxaliplation, we performed 8 concentration gradients. After 72 h in culture, the cell viability was measured using Cell Counting Kit-8 (CCK-8) assays (Dojindo). Each experiment with six replicates was repeated three times.

Processing EIF2S2 knockdown RNA-Seq data

The raw sequencing reads were first processed to trim adapter sequences and low-quality bases by Trimmomatic (Version 0.36)[1]. The parameters was "ILLUMINACLIP: 'Aapter':2:30:10' LEADING:3 TRAILING:3 SLIDINGWINDOW:4:15 MINLEN:36". All filtered reads were aligned to the human reference genome (GRch38) by using the splice-aware aligner HISAT2 with default settings[2]. Next, the alignments were subjected to StingTie[3] program to calculate the gene expression in FPKM units (FPKM = Fragments Per Kilobase of transcript per Million mapped reads). Furthermore, the lncRNAs annotated in GENCODE v28 were adopted to extract lncRNA expression profiles.

Gene set enrichment analysis

To identify the pathways potentially regulated by EIF2S2, we first calculated the expression correlation coefficient for each gene with EIF2S2. All protein coding genes were ranked based on the correlation coefficient. Next, we calculated the enrichment score (*ES*) based on the GSEA. If there were *N* genes in the ranked gene list $\mathrm{L} = \{g_1, g_2, g_3, \ldots, g_N\}$, the ranked score is $\mathrm{RS}(g_j) = r_j$. We first calculated the fraction of gene in pathway H ("hits") weighted by their rank score and the fraction of genes not in S ("misses") present up to a given position *i* in *L*.

$$P_{hit}(H,i) = \sum_{\substack{g_i \in H \\ j \le i}} \frac{|r_j|^p}{N_R}, where\ N_R = \sum_{g_i \in H} |r_j|^p$$

$$P_{miss}(H,i) = \sum_{\substack{g_{j \notin H} \\ j \le i}} \frac{1}{(N - N_I)}$$

The ES score was the maximum deviation from zero of $P_{hit} - P_{miss}$. Moreover, a p-value was calculated for each pathway that includes N_I of genes.

$$p(ES(N,N_I) < ES_{ik}) = \sum_{q=-\infty}^{\infty} (-1)^q \exp\left(-2q^2 {ES_{ik}}^2 n\right),$$

$$n = \frac{(N - N_I)N_I}{N}$$

Where ES_{ik} is the enrichment score for functional pathway *k*, *N* is the number of genes in the ranked list, and N_I the number of genes in the specific functional pathway. P-values were adjusted by false discovery rate (FDR).

References

1. Bolger, AM, Lohse, M, and Usadel, B (2014). Trimmomatic: a flexible trimmer for Illumina sequence data. *Bioinformatics* **30**: 2114-2120.
2. Kim, D, Langmead, B, and Salzberg, SL (2015). HISAT: a fast spliced aligner with low memory requirements. *Nature methods* **12**: 357-360.
3. Pertea, M, Pertea, GM, Antonescu, CM, Chang, TC, Mendell, JT, and Salzberg, SL (2015). StringTie enables improved reconstruction of a transcriptome from RNA-seq reads. *Nature biotechnology* **33**: 290-295.

Supplementary figures

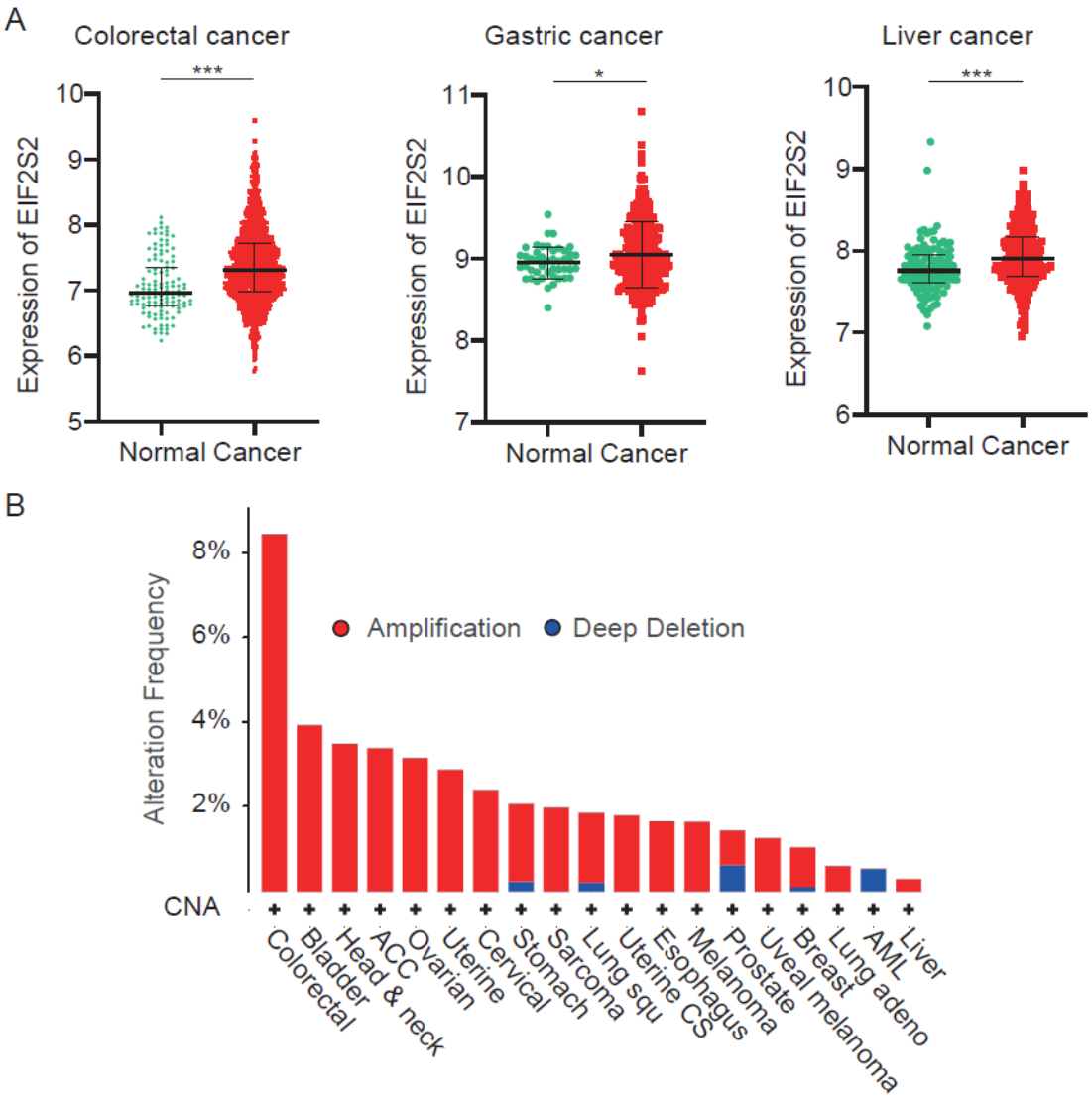

Figure S1. The expression and copy number variation of EIF2S2 in independent data. (A) The expression of EIF2S2 in normal and cancer patients across three cancer types. (B) The copy number alteration frequency of EIF2S2 across different cancer types in TCGA project.

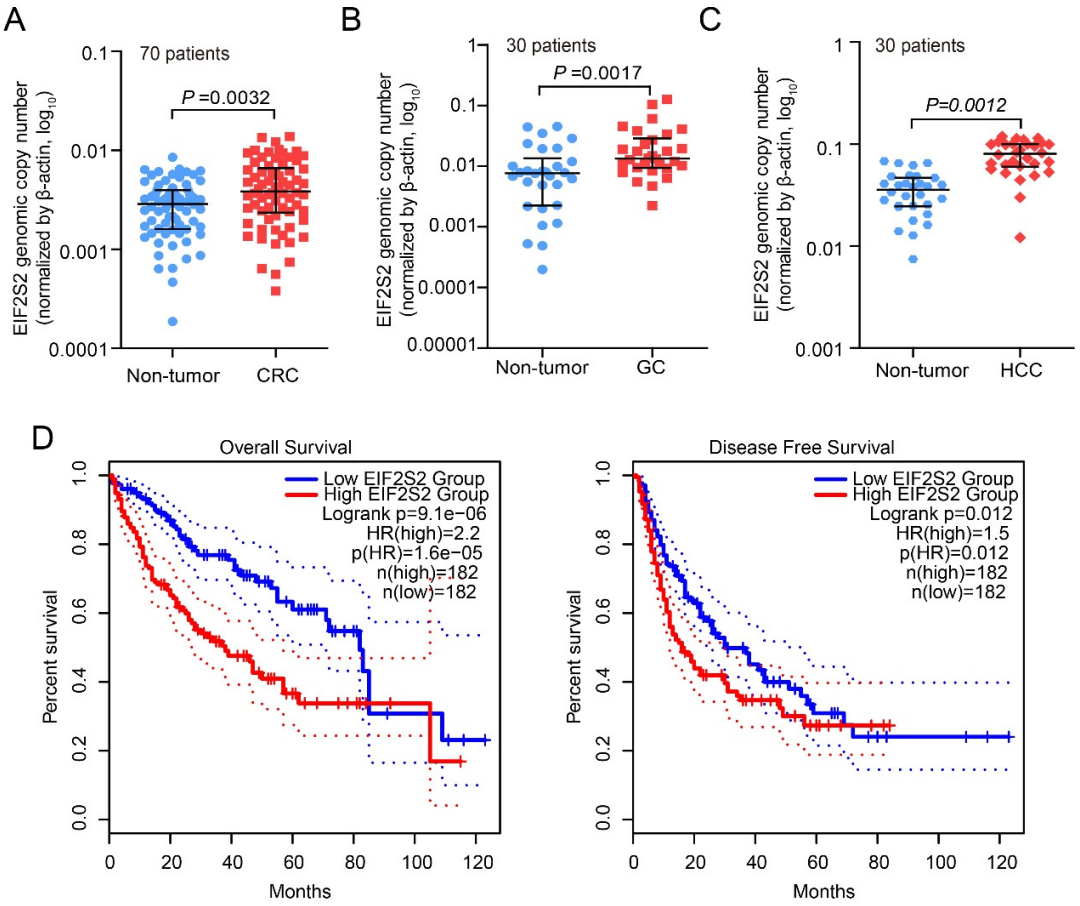

Figure S2. The copy number and clinical association of EIF2S2 in cancer.

(A) The copy numbers of EIF2S2 in 70 pairs of CRC tissues and adjacent normal tissues quantified by q-PCR. (B) The copy numbers of EIF2S2 in 30 pairs of GC tissues and adjacent normal tissues quantified by q-PCR. (C) The copy numbers of EIF2S2 in 30 pairs of HCC tissues and adjacent normal tissues quantified by q-PCR. (D) Kaplan–Meier analyses of the correlation between EIF2S2 RNA levels and the overall survival (left panel) and disease free survival analysis in HCC (right panel).

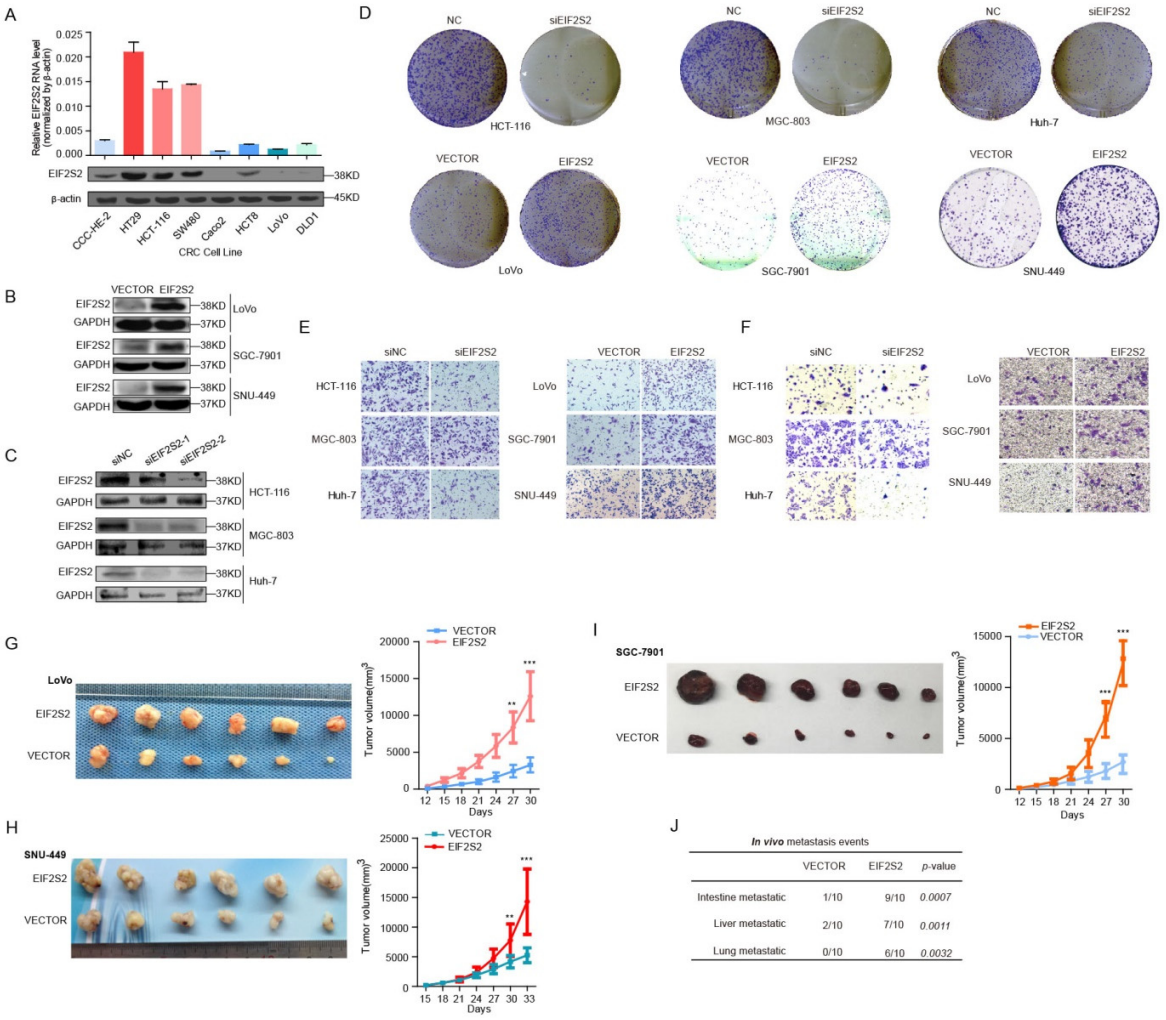

Figure S3. Oncogenetic functions of EIF2S2 in cancer.

(A) RNA levels of EIF2S2 in eight CRC cell lines (top panel), and protein levels of EIF2S2 in eight CRC cell lines (bottom panel). (B) The activation of EIF2S2 by pWPXL-EIF2S2 activation in the LoVo, SGC-7901 and SNU-449 cell lines. (C) The knockout efficiency of EIF2S2 by siRNA in HCT-116, MGC-803 and Huh-7 cell lines. (D) Representative images of colony formation assays in siEIF2S2 or pWPXL-EIF2S2 cancer cell lines. (E) and (F) Representative images of transwell migration and invasion assays for HCT-116 and MGC-803 and Huh-7 cells infected with the siEIF2S2 or the siNC (400×magnification). (G)-(I) Document planes of nude mouse models bearing subcutaneous tumor xenografts from pWPXL-EIF2S2 cells or vector in cell lines. (J) In vivo metastatic events in LoVo cells infected with the lentivirus expressing EIF2S2 or the control.

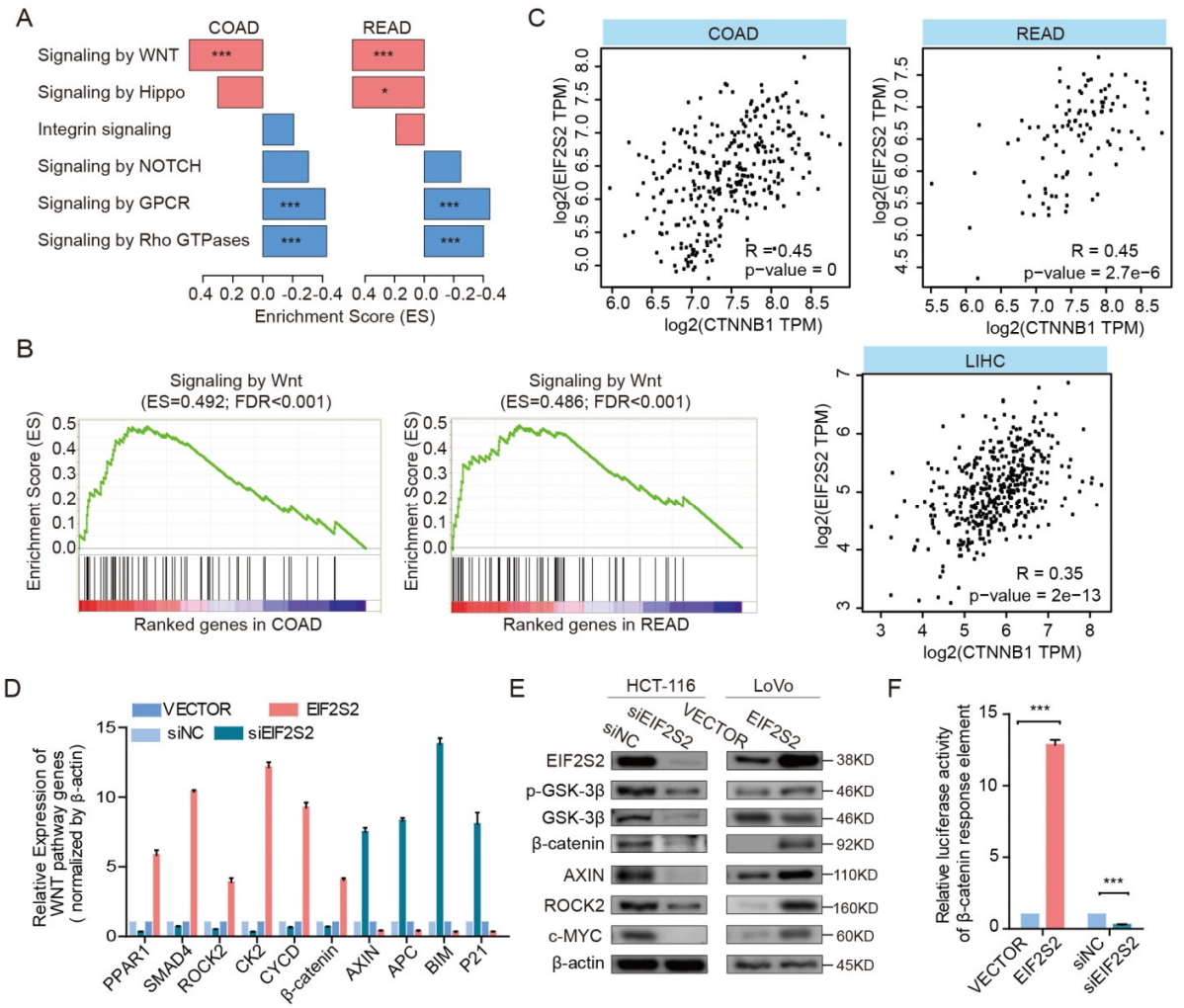

Figure S4. EIF2S2 perturbs Wnt signaling Pathway involved in tumor cell proliferation and metastasis.

(A) The signaling pathways enriched by the genes that co-expressed with EIF2S2. Left panel for COAD and right panel for READ. Red for pathways enriched by positively co-expressed genes and blue for negatively co-expressed genes. (B) GSEA enrichment plots of co-expressed genes with EIF2S2 belonging to the Wnt signaling pathway. The bar-code plot indicates the position of the genes on the expression data rank-sorted by its association with EIF2S2, with red and blue colors indicating positively and negatively co-expressed genes. (C) The scatter plots of the expression of EIF2S2 and CTNNB1 in COAD, READ and LIHC cancers. (D) The mRNA levels of Wnt signaling pathway genes in LoVo cells infected with lentivirus expressing EIF2S2 or transfected with EIF2S2 siRNAs. (E) The protein levels of Wnt signaling pathway genes in LoVo cells infected with lentivirus expressing EIF2S2 or transfected with EIF2S2 siRNAs. (F) Luciferase assays for CRC cells infected with lentivirus expressing EIF2S2 or transfected with EIF2S2 siRNAs. Values are expressed as mean±SEM (n=3). ***p<0.001, Wilcoxon signed-ranks test.

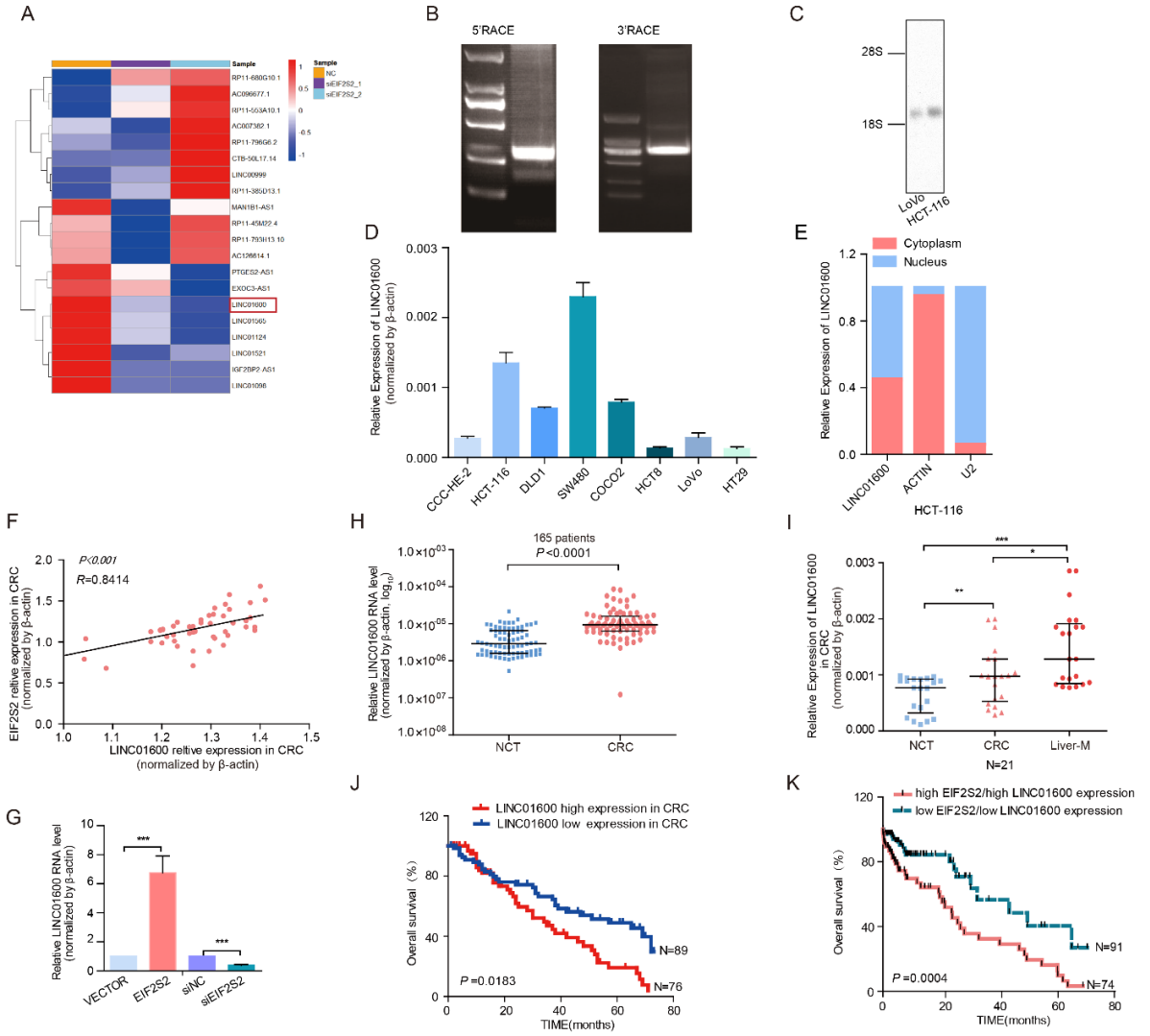

Figure S5. LINC01600 is overexpression in CRC and correlated with patient survival.

(A) Heat map of expression of lincRNAs between HCT-116 cells transfected with EIF2S2 siRNAs or control. (B) Representative images of LINC01600 PCR products from the 5' RACE and 3' RACE. (C) Northern-blotting for LINC01600 in LoVo and HCT-116. (D) The RNA levels of LINC01600 in eight CRC cell lines. (E) The distribution of LINC01600 RNA in HCT-116 cells (cytoplasmic, magenta; nuclear, spearmint). β-actin served as cytoplasmic internal control. U2 served as nuclear internal control. (F) Expression correlation of EIF2S2 and LINC01600 in CRC. (G) Relative expression of LINC01600 in EIF2S2 over-expressing and knockdown cell lines. (H) Relative expression of LINC01600 in 165 CRC patients and adjacent normal control. (I) Relative expression of LINC01600 in normal controls, cancer and liver metastatic patients. (J)

Kaplan–Meier analyses of the correlation between LINC01600 RNA levels and the overall survival in 165 patients with CRC. Patients were stratified for the analysis by the median expression of LINC01600 in CRC patients. (K) Combined influence of EIF2S2 and LINC01600 on the patient survival. The patients with high EIF2S2 expression and high LINC01600 expression showed significantly optimal survival.

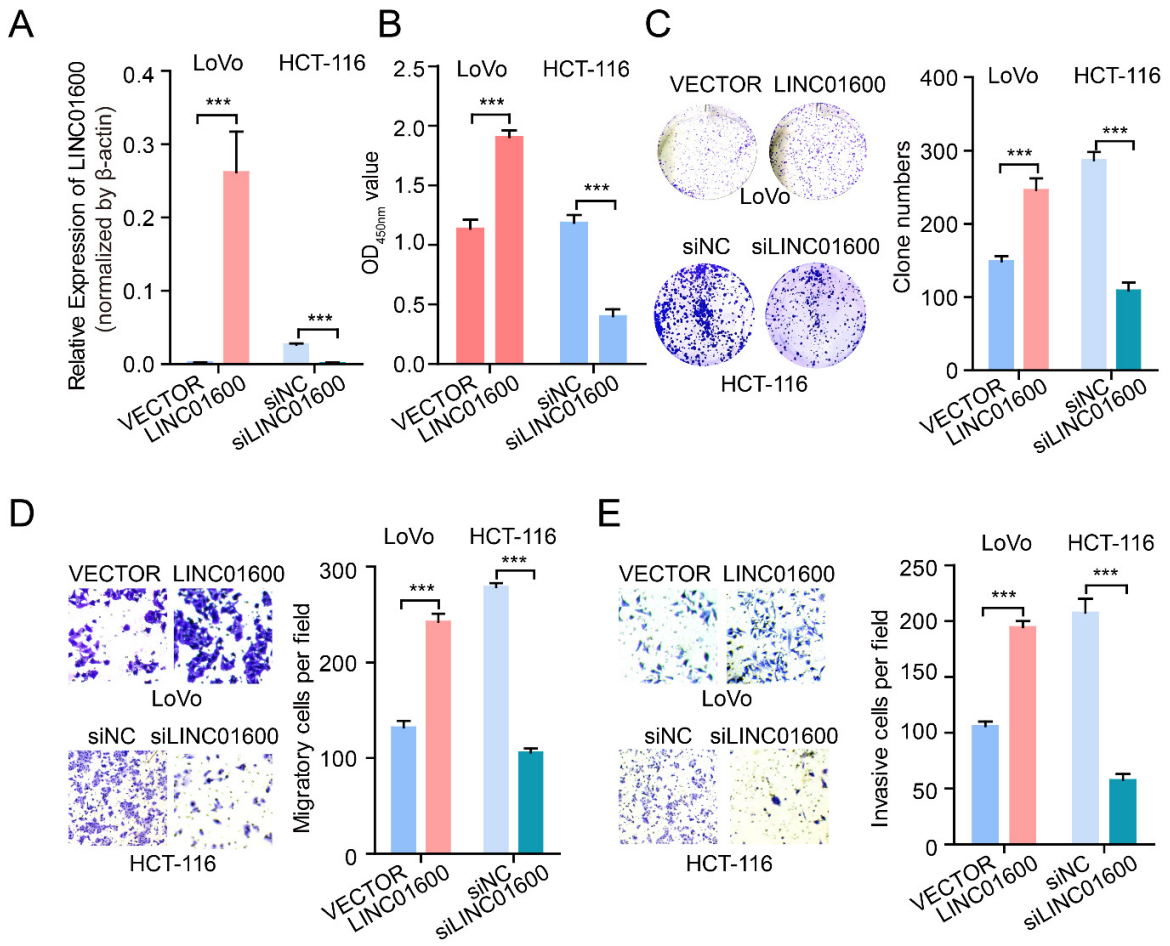

Figure S6. LINC01600 promotes CRC cell proliferation and metastasis in vitro.

(A) The activation of LINC01600 by pWPXL-LINC01600 in the LoVo, and the knockout efficiency of LINC01600 by siRNA in HCT-116 cells. (B)-(E) CCK-8 assays (B), colony formation assays (C), trans-well migration (D) and invasion (E) assays in stable pWPXL-LINC1600 LoVo and siLINC01600 HCT-116 cells. Values are represented as mean+standard error of the mean (SEM), n=3. ***P < 0.001, Wilcoxon signed-ranks test.

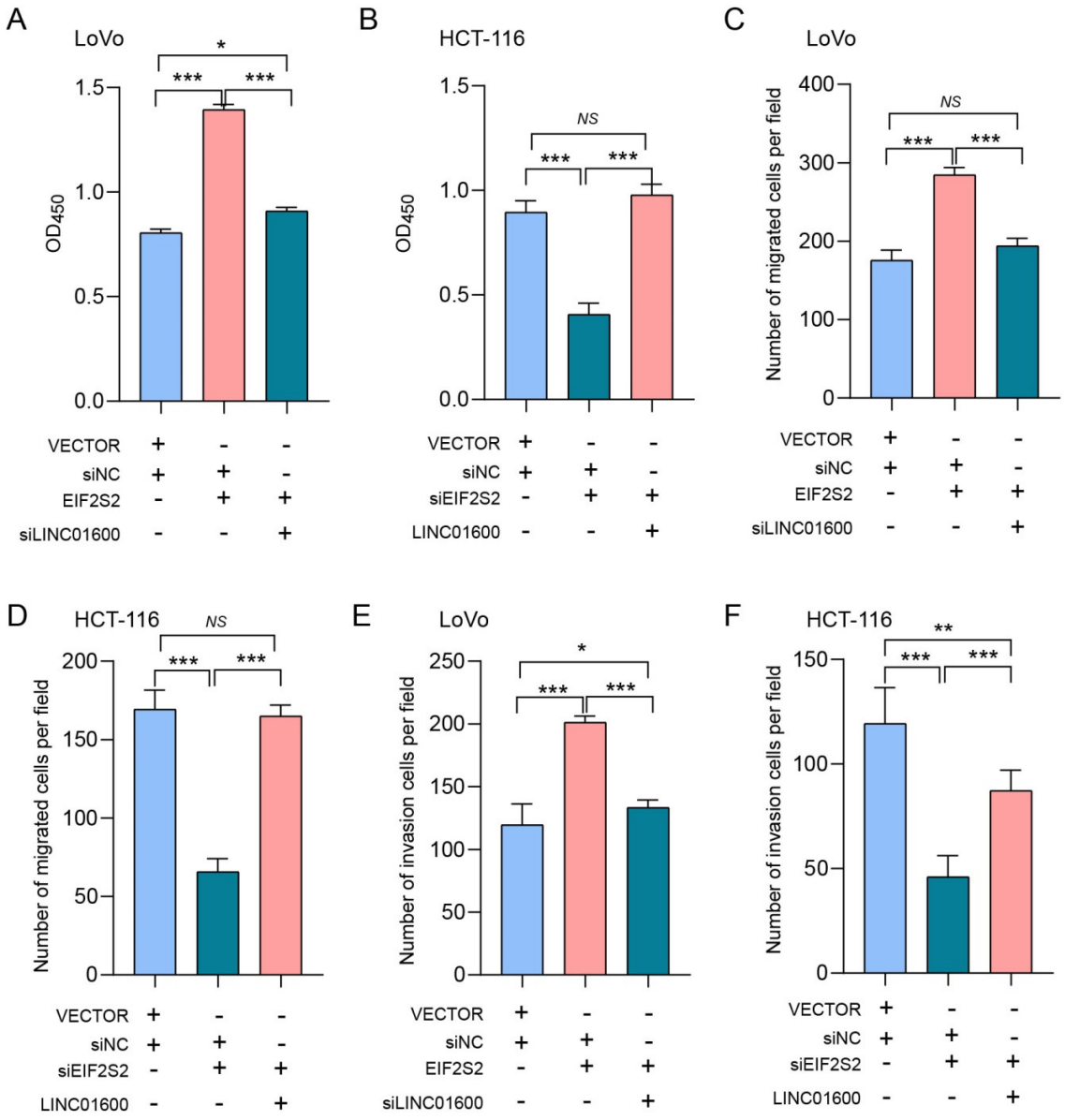

Figure S7. LINC01600 reverse the effects of EIF2S2 on cell proliferation, migration and invasion. (A) and (B), Cell proliferation. (C) and (D), Number of migrated cells per fileld. (E) and (F), Number of invasion cells per field.

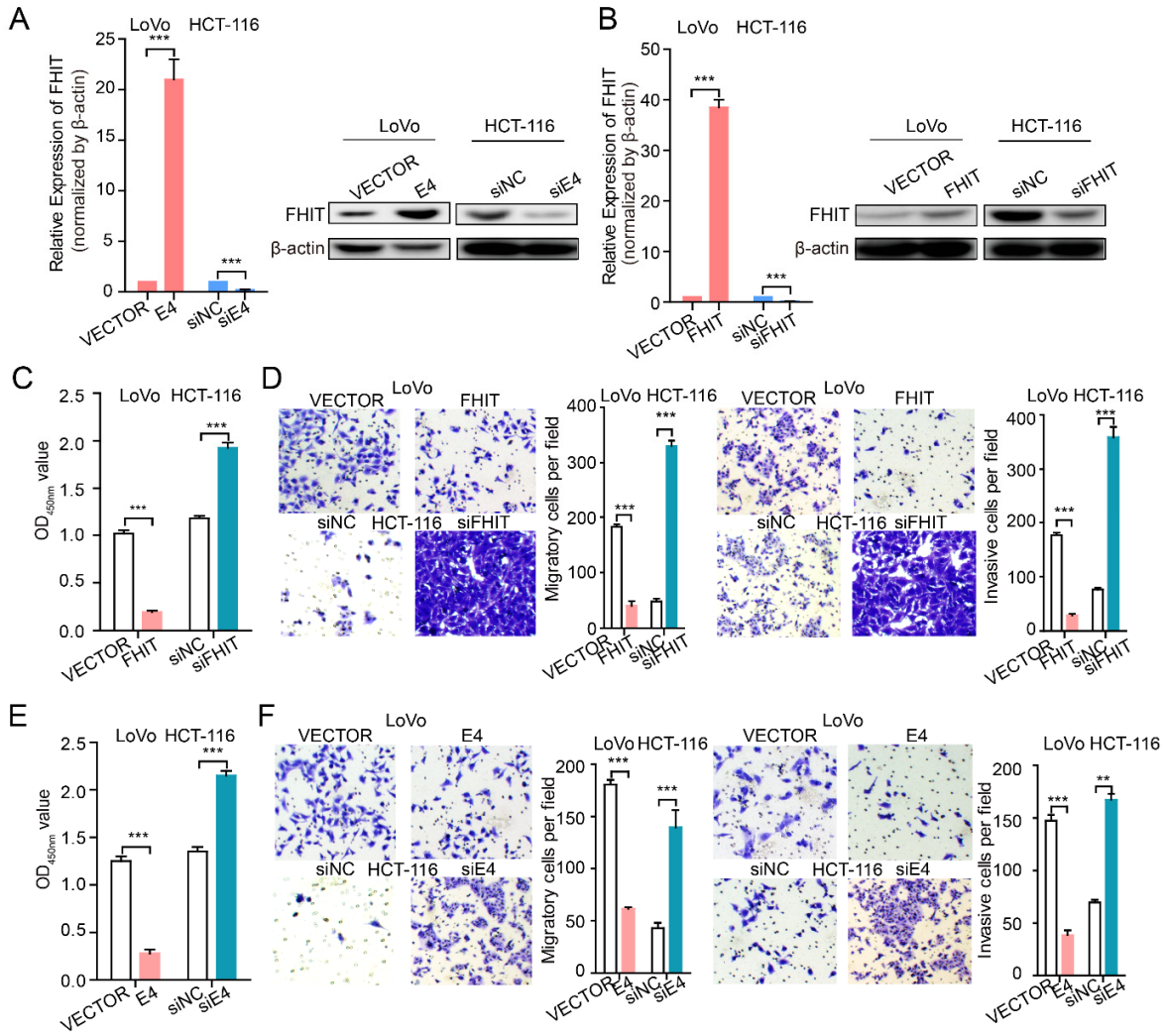

Figure S8. Enhancer E4 and FHIT function in CRC cell proliferation and metastasis in vitro.

(A) qPCR assays measuring FHIT RNA expression by inducing or repressing enhancer activity of E4 in LoVo and HCT-116 (left panels). Immunoblotting analysis FHIT protein expression affected by the enhancer activity of E4 in LoVo and HCT-116 (right panels). (B) qPCR assays measuring the activation of FHIT by pWPXL-FHIT in LoVo, and the knockout efficiency of FHIT by siRNA in HCT-116 cells (left panels). Immunoblotting analysis FHIT protein activation by pWPXL-FHIT in the LoVo, and the knockout efficiency of FHIT by siRNA in HCT-116 cells (right panels). (C) and (D) CCK-8 assays (C), trans-well migration (left panels in D) and invasion (right panels in D) assays in stable pWPXL-FHIT LoVo and siFHIT in HCT-116 cells. (E) and (F), CCK-8 assays (E), trans-well migration (left panels in F) and invasion (right panels in F) assays in stable expressing E4 in LoVo and knock down E4 in HCT-116 cells.

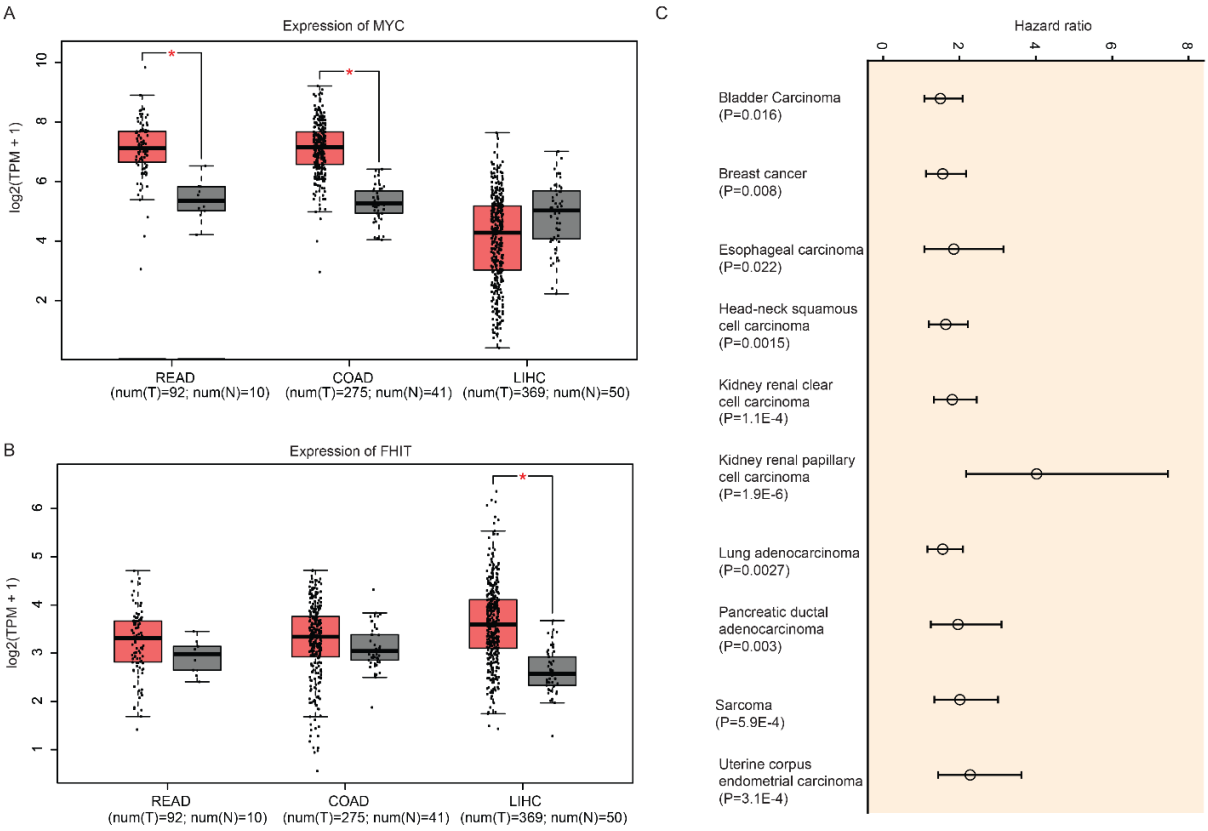

Figure S9. Expression of MYC and FHIT in cancer and clinical association of EIF2S2 across cancer types.

(A) The boxplots show the expression distribution of MYC in READ, COAD and LIHC. (B) The boxplots show the expression distribution of FHIT in READ, COAD and LIHC. (C) The hazard ratio distribution of the association between expression of EIF2S2 and patients' survival across cancer types. The log-rank p-values are shown at the bottom of each cancer type. The error bars showing the 95% confidence level of hazard ratio (HR).

Table S1. Number of cancer types and literature for RBPs. (Table S1.xls)

Table S2. Resource and primers used in this study.

REAGENT or RESOURCE	SOURCE	DENTIFIER
Antibodies		
EIF2S2	Abcam	ab86105
Phospho-GSK3β	Cell Signaling Technology	#5558
GSK3β	Cell Signaling Technology	#5676
β-catenin	Abcam	ab16051
AXIN	Cell Signaling Technology	#2521
ROCK2	Cell Signaling Technology	#9029
c-MYC	Cell Signaling Technology	#5605
β-actin	Cell Signaling Technology	#5125
GAPDH	Cell Signaling Technology	#3683
FHIT	Abcam	ab180806
siRNA sequences		
siEIF2S2	This study	AAGTCGTCCGAGTAGGAACCA
siLINC01600-1	This study	AACGTGGTGGCATCTGCTTGTGG
siLINC01600-2	This study	AAACGGGGTGGCATCCGCTC
siMYC-1	This study	GGTGTGACCGCAACGTAGGA
siMYC-2	This study	ATATCCTCGCTGGGCGCCGG
siMYC-3	This study	AACGTTGAGGGGCATCGTCG
siFHIT-1	This study	TTCTAGGATGGCCCCGAAGC
Cell Lines		
HEK-293T	This study	ATCC
MGC-803	This study	Shanghai Meixuan
SGC-7901	This study	Shanghai Meixuan
LoVo	This study	ATCC
Caco2	This study	ATCC
HT29	This study	ATCC
HCT8	This study	ATCC
HCT116	This study	ATCC
CCH-HE-2	This study	ATCC
DLD1	This study	ATCC
SW480	This study	ATCC
Hu-7	This study	Japanese Collection of Research Bioresources
SNU-449	This study	Shanghai Cell Bank Type Culture Collection Committee
Primers		
Name	Forward-primer	Reverse-primer
EIF2S2-qPCR	CCAGAGCCAACTGAGGACAA	ACATCACTTTCAATCTTTACACCTT
β-actin-qPCR	AGTGTGACGTGGACATCCGCAAAG	ATCCACATCTGCTGGAAGGTGGAC
PAR1-qPCR	TTTCCAGCTTTCCCACCCTC	CATGGGGCTATATCTGGGGC
SMAD4-qPCR	GCTGCAGAGCCCAGTTTAGA	CCCCAAAGCAGAAGCTACGA
ROCK2-qPCR	TCCCGATAACCACCCCTCTT	GGAAAAAGGCTTTCCAGCCG
EIF2S2-OUT	CGGAATTCCGGTGGAGCGTTAATTACA TAAGAGGCACTGAT	CGGGATCCCGTGTGGCGCGAGTTACCAG GCGACGCCGCGTCGCCAGGC
EIF2S2-IN	CGGAATTCCGTCGCCTGG TAACTCGCGCC ACAC	GGACTAGTCCCGGGATCCCGTGGAGCGTT AATTACATAAGAGG
LINC01600-northern	AACGGCCTACAGTGGCTTACAAC	GGACTAGTCCGGAGCCACTCTGCCAGCCA G
LINC01600-sense	GAGCGGATGCCACCCCGTTTCCA	AAGATAAGTAACATTTTTTAATTG
LINC01600-antisense	CAATTAAAAAATGTTACTTATCTT	GAGCGGATGCCACCCCGTTTCCA

MCM3-ORF	AGTCATCCTGGGAACCTCCA	AGTCATCCTGGGAACCTCCA
CDC6-qPCR	AAGGGCGTTGGGGTCATAAG	GGCTTCATCTAAGGGCAGCA
PRRT2-qPCR	CTCCCTCCCTCCCTAGCTG	GAATAGCAGAGACAGCGGCA
CCND1-qPCR	TGAGGGACGCTTTGTCTGTC	GCCTTTGGCCTCTCGATACA
CK2-qPCR	GCCTTTGGCCTCTCGATACA	CAGCTGGGGGTAAGACCTTG
AXIN-qPCR	CAGCTGATCGATCCTGCCAT	ATATGCCCTTCCCTGTCCCT
APC-qPCR	GGAAATTCCCGGGGCAGTAA	GCCTGGTTCATGAGCTTCCT
P15-qPCR	GGGACTAGTGGAGAAGGTGC	CATCATCATGACCTGGATCGC
P21-qPCR	AGCTGCCGAAGTCAGTTCCTT	GTTCTGACATGGCGCCTCCT
BIM-qPCR	GTATTCGGTTCGCTGCGTTC	CGCAGGCTGCAATTGTCTAC
GSK3β-qPCR	GACTAAGGTCTTCCGACCCC	AAGAGTGCAGGTGTGTCTCG
MAPK1-qPCR	ACTTCAGGGGTGCCACATTC	CCTCCCGCAGGGATCTGC
CDKN2A-qPCR	ACTTCAGGGGTGCCACATTC	CGACCCTGTCCCTCAAATCC
CCNT1-qPCR	TAACTCGGCTACGGGGTGTA	CTAAGAGGCGACCCACATCC
HDAC3-qPCR	ATTGCCTCTGGCTTACCTCC	GTCTGGGATTGTGTGAACGC
LINC01600-qPCR	TGGGATGAAGACTCAACGGC	CGGGAGTTGTAAGCCACTGT
FHIT-qPCR	GAAGCCGGACAGACTGTGAA	TGCTGCCATTTCCTCCTCTG
FHIT-S1F1	CGGAATTCCGGCACTGCCACATCCCCACGGTCA	CGGGATCCCGTTTAAAAGCAGCCTGTTTCTGTC
FHIT-S1F2	CGGAATTCCGGGTCTGTGGCCTTGAAAGAGCA	CGGGATCCCGCCCAAGGTCACACAGTTGGT
FHIT-S1F3	CCGCTCGAGCGGGTGGACACAGGCCGGCAGCCATG	GGACTAGTCCTGGCTTCAGCCTGCGGCCTGA
FHIT-S1F4	CGGGATCCCGCCGGGAACAGAGGGCAAAAAGTCCT	GGACTAGTCCGGTCAGTGTTTCCCGCCCC T
FHIT-S1F5	CGGAATTCCGGACATATGCATGCTGTCTGCTTTTAA	CGGGATCCCGACCCTACTGAGATCACAGCTTGGAC

Deposited Data		
TCGA RNA sequencing data	Genomic Data Commons	https://portal.gdc.cancer.gov/
Cancer Cell Line Encyclopedia	The Broad Institute	https://portals.broadinstitute.org/ccle
TCGA clinical data	Genomic Data Commons	https://portal.gdc.cancer.gov/
MYC-ChIP-Seq	Gene Expression Omnibus	GSM1239473
DNase-Seq	ENCODE	ENCSR503BEM_rep1
DNase-Seq	ENCODE	ENCSR503BEM_rep2

Software and Algorithms		
TCGAbiolinks	R Package	https://bioconductor.org/packages/release/bioc/html/TCGAbiolinks.ht ml
Gene Set Enrichment Analysis (GSEA)	Java package	http://software.broadinstitute.org/gsea/index.jsp
R (v3.5.1)	CRAN	https://cran.r-project.org/
ggplot2	R package	https://cran.r-project.org/web/packages/ggplot2/index.html
survival	R package	https://cran.r-project.org/web/packages/survival/index.html
bedtools		https://bedtools.readthedocs.io/en/latest/
liftover	UCSC	http://genome.ucsc.edu/cgi-bin/hgLiftOver
pheatmap	R package	https://cran.r-project.org/web/packages/pheatmap/